Applied Catalysis B: Environmental 102 (2011) 140–146

Contents lists available at ScienceDirect

Applied Catalysis B: Environmental

journal homepage: www.elsevier.com/locate/apcatb

Photocatalytic degradation and detoxification of *o*-chloroaniline in the gas phase: Mechanistic consideration and mutagenicity assessment of its decomposed gaseous intermediate mixture

Taicheng An[a,*], Lei Sun[a,b], Guiying Li[a,*], Yanpeng Gao[a,b], Guangguo Ying[a]

[a] *State Key Laboratory of Organic Geochemistry and Guangdong Key Laboratory of Environmental Resources Utilization and Protection, Guangzhou Institute of Geochemistry, Chinese Academy of Sciences, Guangzhou 510640, China*
[b] *Graduate School of Chinese Academy of Sciences, Beijing 100049, China*

ARTICLE INFO

Article history:
Received 31 August 2010
Received in revised form 8 November 2010
Accepted 24 November 2010
Available online 1 December 2010

Key words:
Volatile organic compounds
O-chloroaniline
Photocatalytic degradation
Detoxification
Degradation mechanism

ABSTRACT

The photocatalytic degradation of *o*-chloroaniline (*o*-ClA) on a TiO_2 thin film was investigated using *o*-ClA as a model of semi-volatile organic compounds. The degradation efficiencies of *o*-ClA with *ca.* 4300 μg L^{-1} were up to 99.0% within a 300 min illumination. The degradation kinetics of *o*-ClA followed a pseudo first-order reaction. Two intermediates, chlorobenzene and phenol, were found in the gas phase, and trace phenol and *o*-dihydroxybenzene were also detected on the surface of the TiO_2 film. Based on the identified intermediates and the theatrical calculation data of the frontier electron densities and point charges, a photocatalytic degradation mechanism was proposed tentatively. When tested using SOS/umu and Ames assay, neither the *o*-ClA nor the gaseous intermediates at different degradation times presented mutagenic activity to strain TA1535/pSK1002(−S9) as well as TA98(±S9) and TA100(−S9) at all tested doses. However, *o*-ClA at high doses did show weak mutagenic activity to strain TA1535/pSK1002 in SOS/umu assay and to strain TA100 in Ames assay with S9 metabolic activation. However, the mutagenic toxicity of the gaseous intermediates decreased rapidly as the degradation time increased, and when tested using both mutagenicity assays, no mutagenic activity was seen after 300 min. Therefore, by combining mechanistic consideration with mutagenicity assessment, photocatalytic technology was found to be an effective detoxification method for gaseous aromatic amines.

1. Introduction

Volatile organic compounds (VOCs) are existed due to widely used in both domestic and industrial activities. However, most VOCs are toxic, mutagenic, and carcinogenic to humans and are therefore detrimental to human health. In fact, long-term exposure to indoor and industrial sources can cause sick building syndromes [1] and occupational diseases [2,3]. Therefore, increasing attention has been paid to the carcinogenic and adverse effects of various VOCs on human health [4,5]. However, most studies have focused on the toxicity of VOCs alone rather than on the degradation intermediates produced during treatment processes [6,7].

Aromatic amines, one kind of VOCs, were first recognized as carcinogenic in 1895 when Ludwig Rehn reported a high incidence of bladder cancer in dye industry workers, as "aniline cancer" [8]. Chloroaniline is a typical semi-volatile aromatic amine present in the air, which is a by-product from the manufacture and processing of coal oil and gasoline [9]. It is also considered by the United States Environmental Protection Agency as an indicative toxic chemical to marine organisms [10]. In recent decades, the degradation of aromatic amines and chloroaniline in the gas phase has received increasing attention because of its adverse effects on human health [11]. However, information on the degradation of gaseous chloroaniline remains limited, although a few studies have been conducted on its degradation in water by biodegradation [12,13] and catalytic oxidation [14–16].

Photocatalytic technology has been repeatedly proven to be a highly effective method for the degradation of a wide spectrum of VOCs in the air [17,18]. Its appeal lies in its potential to mineralize various VOCs into less toxic and less harmless compounds under mild conditions [19]. Current studies are focused on its application feasibility, kinetics aspects, and an attempt to improve its degradation efficiencies by developing new photocatalysts for VOCs abatement [20]. However, the gaseous intermediates produced during the photocatalytic degradation of VOCs should not be ignored because they may result in more toxic gaseous intermediates [11] or can occupy the active sites of the catalyst and lead to the deactivation of such catalyst [20]. Therefore, the identification of

* Corresponding authors. Tel.: +86 20 85291501; fax: +86 20 85290706.
E-mail addresses: antc99@gig.ac.cn (T. An), ligy1999@gig.ac.cn (G. Li).

0926-3373/$ – see front matter © 2010 Elsevier B.V. All rights reserved.
doi:10.1016/j.apcatb.2010.11.035

the produced intermediates and the tentative mechanism involved should be investigated. However, only a few studies have focused on the mutagenicity assessments and detoxification possibilities of VOCs in the air. In particular, only a few have been conducted on the mutagenicity assessments of gaseous mixed intermediates during photocatalytic degradation.

This study aims to examine the detoxification capability of photocatalysis and to evaluate the safe discharge of gaseous aromatic amines as an alternative to the conventional method. *O*-ClA was used as a model of semivolatile organic compounds to probe the gaseous photocatalytic detoxification possibility of aromatic amines. Gas chromatography–mass spectrometry (GC–MS) was used to identify the intermediates both in the gaseous phase and on the surface of the photocatalyst. The possible degradation pathways of *o*-ClA were also analyzed based on the identified intermediates with the assistance of the theatrical calculation data of the frontier electron densities (FEDs) and point charges. Two genotoxicity methods, SOS/umu assay and Ames assay, were employed to confirm the safety discharge of the gaseous degradation intermediate mixture after photocatalytic degradation.

2. Experimental

2.1. Reagents

O-Nitrophenyl-β-D-galactopyranoside (ONPG) was purchased from Amresco Corp. (Solon, USA); sodium dodecyl sulfate (SDS) from Calbiochem Corp. (Bad Soden, Germany); β-Mercaptoethanol, glucose-6-phosphate (purity >98%), dimethyl sulfoxide (purity >99.9%), and dexon (purity 99%) from Sigma Chemical Corp. (Saint Louis, USA); 2-aminofluorene (purity >97.0%) from Fluka Chemical Corp. (Ronkonkoma, USA); N,O-bis (trimethylsilyl)-trifluoroacetamide (BSTFA) (purity >98%) from Acros Organics (New Jersey, USA); and 3,4-benzypyrene (purity >97%) from Tokyo Kasei Kogyo Co., Ltd. Nicotinamide adenine dinucleotide phosphate, D-biotin, L-histidine, agar, nutrient broth, and other chemicals were of analytical grade. Rat liver enzymes (S9) and *Salmonella typhimurium* (*S. typhimurium*) strains, TA98, and TA100 were obtained from the Guangzhou Sanitation Prevention Station, China. The strain TA1535/pSK1002 was supplied by Professor Guangguo Ying from our institute.

2.2. Photocatalytic procedures

The titanium dioxide thin films were prepared *via* our reported method [21]. All photocatalytic experiments were performed in a sealed Pyrex glass gas–solid reactor with a total volume of 5 L [22]. The reaction temperature was maintained at room temperature by a continuous circulation of cooling water in the quartz glass jacket around the light source (light intensity: 5.3 mW cm^{-2}). A mini-type fan stirrer at the bottom was used as the air blender for the reaction gas during the operation. Four identically fabricated TiO_2 films were fixed into the reactor. From the injection port, liquid *o*-ClA and a small fraction of distilled water were injected into the vaporizing tube and heated to vaporize until gas–solid adsorption equilibrium was reached. The photocatalytic degradation of *o*-ClA was carried out with a circulation process using a gas circulation pump joined with Teflon tubing from the bottom to the top of the reactor. The equilibrium concentration of *o*-ClA was 4300 μg L^{-1}, and the relative humidity was *ca.* 45% after a 120 min dark adsorption. Once the concentration of *o*-ClA stabilized, the gas was then irradiated with UV light, signaling the start of the photocatalytic degradation. At given time intervals, a portion of gas was collected and sealed in a 1 L Teflon bag for mechanism studies, and the other portions of the gas were trapped with DMSO solution for mutagenicity assessment.

2.3. Analysis

A gas chromatography (GC) equipped with a flame ionization detector (HP 5890) was used to analyze the gaseous concentrations of *o*-ClA. Then 500 μL gaseous samples were taken and injected into the GC for *o*-ClA determination in splitless mode using a 500 μL gas-tight locking syringe. The concentrations of *o*-ClA were quantified using an external standard calibration. The temperatures of the injector and the detector were set at 250 and 280 °C, respectively. The column temperature program was as follows: initially 40 °C for 2 min, programmed to 100 °C at a rate of 6 °C min^{-1}, and then to 280 °C at a rate of 10 °C min^{-1}. The generated gaseous intermediates were analyzed using a Thermo Trace GC Ultra-DSQ II mass spectrometer detector (MSD) with a DB-5 capillary column (30 m × 0.32 mm × 0.25 μm). The analysis method and programmed procedure were the same as the GC quantification. The MSD was operated in full scan mode with m/z 40–300 amu, and the gaseous intermediates were identified via their mass spectrum using the Wiley Mass Spectral Library.

The trace intermediates absorbed on the surface of the TiO_2 film were extracted ultrasonically using a small amount of methanol for 30 min. The extract was filtered through a 0.45 μm filter membrane and collected, concentrated with a gentle stream of high-purity nitrogen, divided into half in two vials, and then completely dried with a gentle stream of high-purity nitrogen. One was re-dissolved with 1.0 mL ethyl acetate and then injected into the GC–MSD for the direct determination of intermediates, whereas the other was derivatized at room temperature with 50 μL BSTFA as the derivatization reagent with 50 μL pyridine catalyst for the determination of polar intermediates produced during the photocatalytic degradation because the trimethylsiloxane derivatized intermediates possess high evaporation performance than underivatized one in GC. Then 1.0 μL resultant solution was injected into the GC–MSD in splitless mode for the indirect identification of polar intermediates. The intermediates were identified *via* their mass spectrum according to the library spectra, and all the identified intermediates were confirmed using authentic standard reagents.

2.4. Calculation of frontier electron densities and point charges

Molecular orbital calculations were carried out using Gaussian 03 program (Gaussian, Inc.) at the single determinant (HF/3-21) level with the optimal conformation having a minimum energy obtained at the B3LYP/6-31G* level. The frontier electron densities (FEDs) of the highest occupied molecular orbital (HOMO) and the lowest unoccupied molecular orbital (LUMO) were calculated. The values of $2FED^2_{HOMO}$ and $(FED^2_{HOMO} + FED^2_{LUMO})$ were obtained to predict the reaction sites for electron extraction and •OH radical attack, respectively [23,24]. Natural bond orbital (NBO) analysis is a good technique for studying hybridization and covalency effects in polyatomic wave functions, based on local block eigenvectors of the one-particle density matrix. In this paper, the NBO calculational results could reveal the distribution of point charges on the skeletal atoms to predict the chemisorption position of *o*-ClA onto the TiO_2 film [25]. All calculations were performed on a personal computer.

2.5. Mutagenicity assessment

The SOS/umu assays were carried out according to the procedure of Oda et al. [26] and international requirements by ISO [27]. Briefly, the overnight TA1535/pSK1002 bacterial culture was diluted with fresh tryptone glucose ampicillin medium, incubated at 37 °C for 2 h with shaking until the bacteria reached the exponential growth phase. The 96-well microplate was incubated for 2 h at 37 °C, and then the optical density (600 nm) of each microplate well was measured to quantify growth inhibition during the expo-

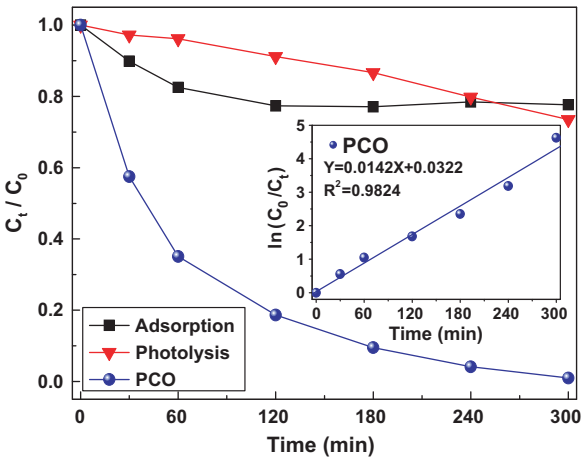

Fig. 1. Photocatalytic degradation kinetics of *o*-ClA. Inset: Linear plots of $\ln(C_0/C_t)$ versus degradation time.

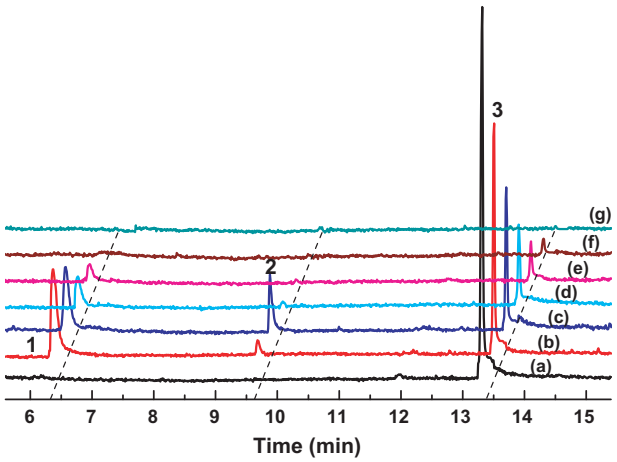

Fig. 2. TIC profile for gaseous compounds photocatalytic degradation of *o*-ClA: (a) 0 min; (b) 30 min; (c) 60 min; (d) 120 min; (e) 180 min; (f) 240 min; (g) 300 min.

sure (toxicity assay). DMSO was used as a solvent control, and 4-NQO and 3,4-benzypyrene were used as the positive control regents without S9 (−S9) and with S9 (+9) metabolic activation, respectively. All samples and solvent blanks were tested in triplicate. Genotoxicity was detected by measuring the activation of SOS response in the bacteria by recording β-galactosidase activity from the integrated reporter system. To avoid interferences, genotoxic effect was quantitatively expressed as induction ratios (IRs), which were calculated for each dose as the ratio of β-galactosidase activity in a sample to the solvent control. IRs above 2.0 were interpreted as sufficient positive results if they had a reproducible dose-response curve, whereas those below 2.0 were interpreted as negative results [28].

Ames assays were performed according to the standard plate incorporation method with *S. typhimurium* classical strains TA98 and TA100, which are capable of detecting base frameshift type and base pair substitution-type mutagenicity, respectively [29]. *O*-ClA and its degradation intermediates at 30, 60, 120, 180, 240, and 300 min were trapped into 5 mL DMSO for mutagenicity test. Four different dose groups (4000, 2000, 1000, and 500 μg plate^{-1}) with the same level as the SOS/umu assay were set up for each sample too. The detailed test procedure and accounting methods for the Ames test were described in our previously published work [30].

3. Results and discussion

3.1. Photocatalytic degradation kinetics

The photocatalytic degradation kinetics of *o*-ClA was investigated, and the results are shown in Fig. 1. *O*-ClA can be photolyzed very slowly under UV light irradiation in the absence of TiO_2. However, in the presence of TiO_2, *o*-ClA was fully eliminated with a degradation efficiency of 99.0% within 300 min. The linear plot of $\ln(C_0/C_t)$ versus time for photocatalytic degradation is shown in the inset of Fig. 1. It indicated that the photocatalytic degradation of *o*-ClA followed a pseudo first-order reaction, and the degradation reaction can be simplified as follows: $\ln C_0/C_t = kt$, which is also consistent with the Langmuir–Hinshelwood (L–H) model [31], where k is the apparent rate constant, t is the degradation time in minute, C_0 and C_t are the initial and the rest concentration of *o*-ClA, respectively. The rate constant, the slope of the linear fit of $\ln(C_0/C_t)$ versus time, was calculated as 0.0142 min^{-1}, and the photocatalytic degradation half-life was also calculated as 49.50 min. The lower rate constant and longer half-life obtained at the same conditions indicate that *o*-ClA was more difficult to be degraded than toluene [22].

3.2. Intermediates identification and degradation mechanism

The degradation of the gaseous mixtures during photocatalysis was subject to GC–MSD analysis for mechanism investigation. The total ion current (TIC) profiles of the gaseous mixture recorded at different reaction times are shown in Fig. 2. Among the samples, only a peak (3) with a retention time (t_R) of 13.29 min was observed before degradation (Fig. 2a) for the original *o*-ClA. The concentration of *o*-ClA dropped rapidly with an increase in degradation time, which indicated that *o*-ClA could be degraded effectively. After a 30 min photocatalytic degradation, peaks 1 (t_R = 6.16 min) and 2 (t_R = 9.47 min) were detected in the gas phase. Identified by mass spectrum analysis (Fig. 3), a couple m/z values of 112/114 were corresponding to the molecule ion peak of chlorobenzene and its isotope peak of 37Cl. And a peak value of 77 corresponding to the phenol ring could also easily find in fragmentation of the mass spectrum of intermediates 1. Also, an m/z value of 94 corresponding to M^+-1 fragmentation of intermediates 2 also was obtained with a molecule weight of phenol. Of course, both the MS cleavage patterns of intermediates 1 and 2 also conform to that of toluene and phenol very well. Thus, the peaks 1 and 2 were assigned as chlorobenzene and phenol, respectively. As the reaction time increased to 60 min, the peak of chlorobenzene decreased slightly, whereas the peak of phenol still increased to its maximum. When the degradation time was further increased, the peaks of both intermediates decreased dramatically and were below the detection

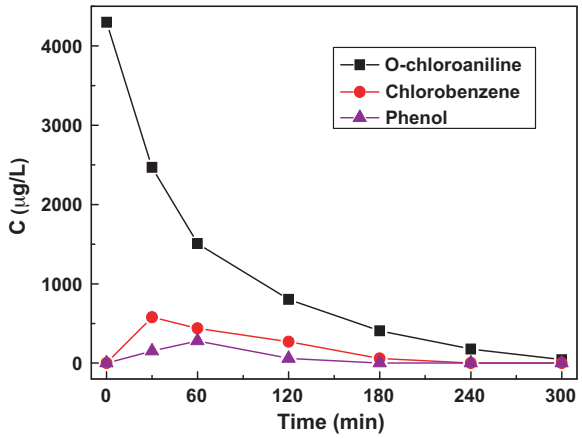

Fig. 3. The mass spectra of detected intermediates in gaseous: (a) chlorobenzene, (b) phenol and (c) *o*-ClA.

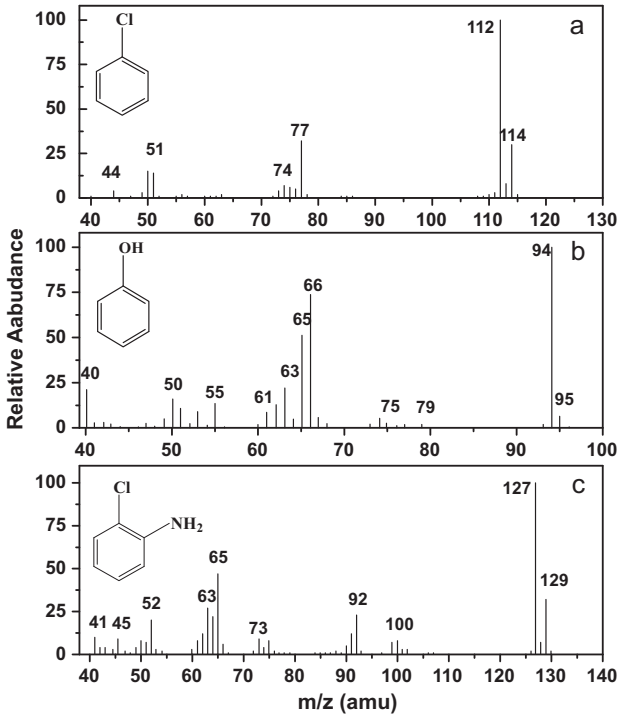

Fig. 4. Concentration change curves for *o*-ClA, chlorobenzene, and phenol in the gas phase.

limit after 240 min. The gaseous intermediates of chlorobenzene and phenol were produced and then subsequently degraded during the degradation course. The concentration changes of the original *o*-ClA and the two intermediates, chlorobenzene (CB) and phenol, with the reaction time are also shown in Fig. 4. As seen in the figure, the original concentration of *o*-ClA with 4300 $\mu g\,L^{-1}$ decreased insignificantly to 2470 and 42 $\mu g\,L^{-1}$ within 30 and 300 min, respectively. On the other hand, the concentrations of chlorobenzene and phenol reached 580 and 150 $\mu g\,L^{-1}$ within 30 min, respectively, and cannot be detected within 300 min. Thus, *o*-ClA and two gaseous intermediates may be completely mineralized into CO_2 and H_2O with enough degradation time.

To gain insight into the produced polar and nonvolatile intermediates involved in the reaction process, the trace solid intermediates adsorbed onto the TiO_2 films were also identified by GC–MSD with and without BSTFA derivatization after methanol extraction. Phenol was also identified in the extracted sample without derivatization, whereas *o*-dihydroxybenzene was detected in the extracted sample with derivatization. The mass spectra of the two solid intermediates are shown in Fig. 5a and b, respectively. As shown in Fig. 5b, the experimentally detected mass spectra as well as the cleavage patterns of bis(trimethylsilyl) derivative of 1,2-dihydroxybenzene was completely conform to that of the authentic standard, 1,2-dihydroxybenzene, bisTMS ether. Thus we can safely confirm the identification of1,2-dihydroxybenzene with derivatization method in this paper.

Photo-induced electrons and holes can be created during photocatalysis when TiO_2 is illuminated by UV light. These photo-induced holes (h^+) can further react with water molecules to form hydroxyl radicals (•OH), whereas the photo-induced electrons can also capture with molecule oxygen to form other weak radicals [31]. Therefore, in the photocatalytic degradation process, active •OH and photoholes are mainly involved in the degradation of *o*-ClA [32].

Theoretically calculated FEDs are recognized as a useful tool to predict initial reaction steps [23,33]. Therefore, the FEDs of *o*-

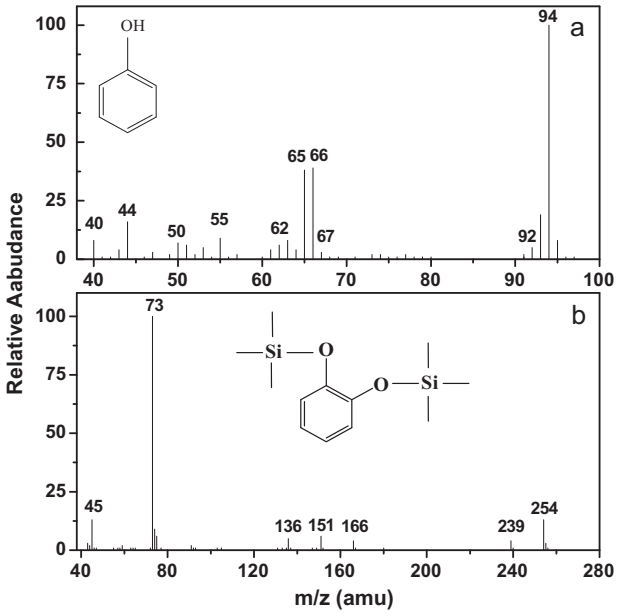

Fig. 5. The mass spectra of adsorbed intermediates onto TiO_2 film identified by GC–MS (a) without and (b) with BSTFA derivatization.

ClA were also calculated to predict the reaction sites for electron extraction (by photohole) and hydroxyl radical attack; the results are summarized in Table 1. According to the Frontier Orbital Theory, the hydroxyl radical is preference to add at positions with a higher $FED^2_{HOMO} + FED^2_{LUMO}$ value, whereas an electron can easily be extracted at positions with higher values of $2FED^2_{HOMO}$ [24]. Thus, for •OH attacks, C^1 (0.3378), C^3 (0.3734), C^4 (0.4243), and C^6 (0.3867) with high ($FED^2_{HOMO} + FED^2_{LUMO}$) values are also likely to be the initial reaction sites, whereas higher $2FED^2_{HOMO}$ values were obtained for C^2 (0.3003) and N^7 (0.3989), indicating that the initial h^+ attacks are likely to occur on these two atoms. On the other hand, point charges can be used to predict the chemisorption position of organics onto TiO_2 [25]. Thus, the point charges of *o*-ClA are also calculated and are shown in Table 1. As seen in the table, the point charge on atom N^7 is by far more negative than those on all others atoms. Therefore, the point of chemisorption of *o*-ClA would be through-NH_2.

Considering that photocatalytic mineralization is initiated by surface-bound •OH radical species and that these species are highly electrophilic, we expect that the primary position(s) for •OH attack

Table 1
FEDs and point charges for *o*-ClA using Gaussian 03 Program.

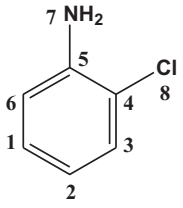

Atom	$2FED^2_{HOMO}$	$(FED^2_{HOMO} + FED^2_{LUMO})$	Point charge
C^1	0.0473	0.3378	−0.314
C^2	0.3003	0.1515	−0.315
C^3	0.0310	0.3734	−0.139
C^4	0.2053	0.4243	−0.118
C^5	0.1836	0.0921	0.323
C^6	0.1370	0.3867	−0.167
N^7	0.3989	0.2022	−0.792
Cl^8	0.0843	0.0661	0.039

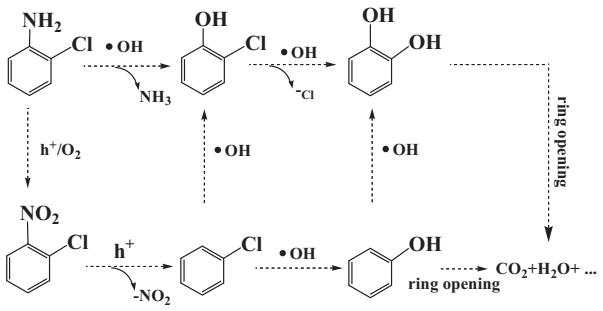

Fig. 6. Proposed photocatalytic degradation pathways for *o*-ClA.

will be on those atoms with the largest electron density. However, the magnitudes of the FEDs are not necessarily reflected by equivalent magnitudes of the negative point charges. For example, the highest electron density in *o*-ClA is at C^4, and yet the point charge on this carbon is only −0.118. Therefore, considering the electron density and the point charge on each atom of *o*-ClA, •OH can replace the amino-group of *o*-ClA to form chlorophenol (CP) (see Fig. 6). This step has also been proposed by Choy *et al.* in water reactions [34]. As observed from Fig. 5, *o*-dihydroxybenzene was identified onto TiO_2 films from the decay of CP by Cl abstraction, which has also been proposed by Bandara et al. by further degradation of CP [35]. Subsequently, the produced *o*-dihydroxybenzene may dissociate two hydrogen atoms to give *o*- benzoquinone (BQ). Further decay of BQ was verified to initiate the formation of a ring cleavage, leading to the production of short chain organic acids. In addition, the formation of inorganic ions (NH_4^+, NO_3^-, and Cl^-) as end-products has also been reported in many previous studies [34].

On the other hand, the reaction may be initiated by the attack of h^+ to *o*-ClA. Based on $2FED^2_{HOMO}$, C^2 and especially N^7 atoms were found to have high values of *o*-ClA. Thus, by combining the results of the FEDs with point charges, the N^7 atom should be the attacked site by h^+ because the reactions with the photohole attacked only took place at the surface of the photocatalysts. Thus, 2-nitrochlorobenzene (NCB) may be produced in subsequent reactions, as shown in Fig. 6, although this intermediate cannot be found in gaseous degradation. However, many studies have been conducted on a similar reaction route of hole-oxidation reactions in aqueous solutions [36]. The resulting NCB can be further oxidized to CP *via* a two-step reaction involving the transformation of CB and then be oxidized to *o*-dihydroxybenzene *via* a two-step reaction involving the transformation of phenol. Finally, phenol and o-dihydroxybenzene can be decontaminated with the opening of aromatic rings and be mineralized into CO_2 and H_2O. Thus, from the viewpoint of chemical analysis, although the identified intermediates both from the gas phase and the adsorbed phase are complicated, all intermediates were detoxified into less toxic pollutants and then would be finally mineralized into CO_2 and H_2O. However, before complete mineralization, some carcinogenic intermediates still need to be seriously considered due to their adverse effects on human health. Therefore, mutagenicity assessment of mixed gaseous intermediates during photocatalytic degradation is still necessary before they complete discharge into the air.

3.3. Mutagenicity assay of gaseous intermediates

Considering that gaseous intermediates can directly endanger human health *via* their inhalation and exposure, both SOS/umu assay and Ames assay were comparatively employed to evaluate the detoxification capability of photocatalysis at different intervals. The SOS/umu assay is one of the short-term genotoxicity tests

Table 2
Results of SOS/umu assay of gaseous intermediates during photocatalytic degradation of *o*-ClA.

Sample	Dose ($\mu g\,\mu L^{-1}$)	IU[a]		IR[b]	
		−S9	+S9	−S9	+S9
o-ClA	0.25	1.34	0.99	1.30	1.24
	0.5	1.14	1.30	1.11	1.62
	1.0	1.06	1.54	1.03	1.92
	2.0	1.50	1.82	1.45	2.27
PCO 30 min	0.25	1.24	0.80	1.20	1.00
	0.5	1.55	0.88	1.50	1.10
	1.0	1.39	0.96	1.35	1.21
	2.0	0.88	1.50	0.85	1.87
PCO 60 min	0.25	1.52	1.20	1.47	1.49
	0.5	0.95	0.94	0.92	1.18
	1.0	1.55	1.09	1.50	1.36
	2.0	1.47	1.10	1.43	1.37
PCO 120 min	0.25	1.18	0.67	1.14	0.84
	0.5	1.11	0.89	1.08	1.11
	1.0	1.33	0.88	1.29	1.10
	2.0	1.35	1.05	1.31	1.31
PCO 180 min	0.25	1.39	0.88	1.35	1.10
	0.5	1.09	0.99	1.06	1.24
	1.0	1.12	1.09	1.09	1.36
	2.0	1.28	0.91	1.24	1.14
PCO 240 min	0.25	1.55	0.70	1.50	0.88
	0.5	0.95	0.79	0.93	0.99
	1.0	1.47	1.00	1.43	1.25
	2.0	1.16	0.78	1.13	0.98
PCO 300 min	0.25	1.13	0.86	1.10	1.1
	0.5	1.12	0.93	1.09	1.16
	1.0	1.33	0.82	1.29	1.0
	2.0	1.18	0.93	1.14	1.16
					Solventcontrol
DMSO	4 μL/well	1.03	0.8	1.0	1.0
					Positivecontrol
2-NQO	1×10^{-3}	12.66		12.29	
3,4-BAP	1×10^{-3}		3.89		4.86

[a] β-Galactosidase activity.
[b] Induction ratio.

for the detection of DNA damage, which is a simple colorimetric assay for the induction of the umuC gene in SOS responses [37]. The tested results of the SOS/umu assay are shown in Table 2. The IR value of *o*-ClA was 1.45 for strain TA1535/pSK1002 without S9 mixture metabolic activation (−S9) at the highest dose of 2000 $\mu g\,L^{-1}$, which indicated that *o*-ClA did not cause mutagenicity to organisms without S9 metabolic activation. After a 30, 60, 120, 180, 240, and 300 min degradation, the IR values were all still less than 2 for strain TA1535/pSK1002 without S9 in all tested dose groups of 2000, 1000, 500, and 250 $\mu g\,L^{-1}$. The same negative results were also obtained with S9 mixture metabolic activation, except for the tested dose of 2000 $\mu g\,L^{-1}$. This indicated that *o*-ClA could cause mutagenicity at this dose in the presence of S9 metabolic activation. Fortunately, all IR values were all lower than 2 for TA1535/pSK1002 after all photocatalytic degradation intervals. That is, *o*-ClA can be photocatalytically decomposed to less mutagenic intermediates during degradation, and the produced mixed gaseous intermediates never obtain positive mutagenicity results to TA1535/pSK1002 with S9 metabolic activation, even when the tested dose is as high as 2000 $\mu g\,L^{-1}$. In order to illustrate clearly the detoxification capability of photocatalytic technology at different degradation intervals, the histogram of IR values at four test doses to TA1535/pSK1002 (+S9) is shown in Fig. 7. As seen from the figure, the mutagenic toxicity of TA1535/pSK1002 (+S9) decreased rapidly with an increase of the degradation time.

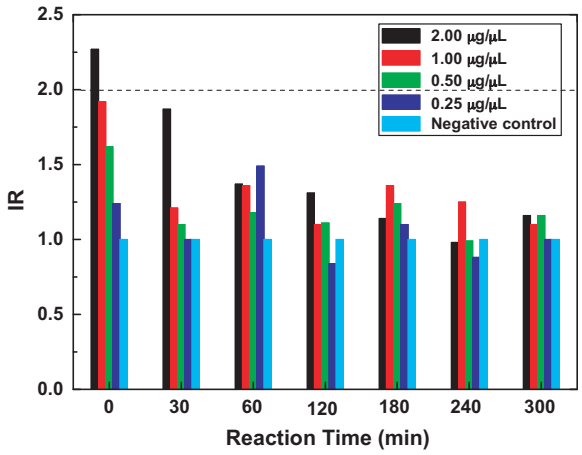

Fig. 7. The values of IR to TA1535/pSK1002 (+S9) at different tested doses of raw *o*-chloroaniline and intermediates at different degradation intervals.

The Ames assay is a convenient and useful tool to compare genotoxic activity by location, meteorological conditions, sources, and other modifying conditions [38]. Thus, the Ames assay was also used to confirm further the mutagenicity of the gaseous intermediates during photocatalytic degradation, because the SOS/umu assay is not as sensitive to most organic pollutants. The relative tested results using Ames assays are also summarized in Table 3. As seen in the table, the range of spontaneous reversions for strains TA98 and TA100 without S9 was 27–33 and 125–132 revertants per plate, respectively, whereas the spontaneous reversions were slightly higher for both strains with S9 activation. For *o*-ClA, at the highest tested dose of 4000 μg plate^{-1}, the number of revertants per plate obtained was 25 ± 3.6 (−S9) (MI = 0.8) and 38 ± 3.8 (+S9) (MI = 1.0) for strain TA98. This means that no obvious increase in the number of revertants was found for TA98 compared with the negative control. However, the number of revertants per plate obtained was 125 ± 4.4 (−S9) (MI = 0.9) and 378 ± 10.6 (+S9) (MI = 2.8) for strain TA100. This indicates that *o*-ClA has a weak mutagenic activity against strain TA100 with S9 because the MI value is greater than 2 at the 4000 μg plate^{-1}, and it had a reproducible dose-response

Table 3
Results of the Ames assay of gaseous intermediates during photocatalytic degradation of *o*-ClA.

Sample	Dose (μg plate^{-1})	Number of revertants plate^{-1} in *S. typhimurium*[a]			
		TA98		TA100	
		−S9	+S9	−S9	+S9
o-ClA	0[b]	31 ± 2.1	37 ± 2.6	132 ± 6.0	136 ± 3.5
	500	30 ± 2.1 (1.0)	41 ± 2.3 (1.1)	127 ± 8.0 (1.0)	139 ± 2.1 (1.0)
	1000	33 ± 2.6 (1.1)	38 ± 4.0 (1.0)	130 ± 4.7 (1.0)	184 ± 5.0 (1.4)
	2000	31 ± 3.1 (1.0)	39 ± 1.7 (1.1)	133 ± 6.5 (1.0)	277 ± 6.7 (2.0)
	4000	25 ± 3.6 (0.8)	38 ± 3.8 (1.0)	125 ± 4.4 (0.9)	378 ± 10.6 (2.8)
PCO 30 min	0	33 ± 3.6	39 ± 2.1	126 ± 4.9	135 ± 2.7
	500	32 ± 1.7 (1.0)	36 ± 1.5 (0.9)	129 ± 9.9 (1.0)	136 ± 2.5 (1.0)
	1000	29 ± 3.2 (0.9)	37 ± 1.2 (0.9)	127 ± 7.0 (1.0)	168 ± 5.3 (1.2)
	2000	32 ± 4.0 (1.0)	35 ± 4.2 (0.9)	131 ± 5.5 (1.0)	205 ± 10.3 (1.5)
	4000	28 ± 2.1 (0.8)	34 ± 2.0 (0.9)	130 ± 6.8 (1.0)	324 ± 7.2 (2.4)
PCO 60 min	0	29 ± 1.2	34 ± 4.0	131 ± 6.1	137 ± 2.5
	500	31 ± 3.1 (1.1)	36 ± 2.6 (1.1)	127 ± 6.0 (1.0)	138 ± 3.8 (1.0)
	1000	28 ± 3.6 (1.0)	34 ± 5.5 (1.0)	127 ± 2.6 (1.0)	141 ± 6.1 (1.0)
	2000	30 ± 5.7 (1.0)	33 ± 2.6 (1.0)	129 ± 3.5 (1.0)	140 ± 7.5 (1.0)
	4000	31 ± 4.4 (1.1)	36 ± 3.1 (1.1)	127 ± 5.0 (1.0)	215 ± 8.9 (1.6)
PCO 120 min	0	28 ± 3.8	38 ± 3.1	130 ± 7.1	139 ± 5.1
	500	30 ± 4.7 (1.1)	38 ± 2.6 (1.0)	127 ± 8.3 (1.0)	136 ± 3.2 (1.0)
	1000	29 ± 5.0 (1.0)	38 ± 5.0 (1.0)	127 ± 4.9 (1.0)	139 ± 5.1 (1.0)
	2000	31 ± 5.5 (1.1)	35 ± 4.6 (0.9)	128 ± 5.7 (1.0)	134 ± 7.8 (1.0)
	4000	30 ± 3.6 (1.1)	38 ± 1.5 (1.0)	125 ± 6.4 (1.0)	190 ± 6.5 (1.4)
PCO 180 min	0	27 ± 2.3	33 ± 3.2	125 ± 3.1	134 ± 5.5
	500	31 ± 2.5 (1.1)	36 ± 4.0 (1.1)	128 ± 2.5 (1.0)	137 ± 10.5 (1.0)
	1000	30 ± 2.5 (1.1)	31 ± 2.6 (0.9)	132 ± 8.1 (1.1)	140 ± 2.1 (1.0)
	2000	29 ± 1.0 (1.1)	34 ± 4.4 (1.0)	128 ± 6.1 (1.0)	140 ± 5.1 (1.0)
	4000	27 ± 4.2 (1.0)	35 ± 2.9 (1.1)	126 ± 3.6 (1.0)	139 ± 3.6 (1.0)
PCO 240 min	0	28 ± 3.2	32 ± 3.6	127 ± 8.1	134 ± 4.6
	500	29 ± 1.0 (1.0)	34 ± 4.9 (1.1)	124 ± 3.5 (1.0)	136 ± 3.5 (1.0)
	1000	27 ± 4.2 (1.0)	31 ± 2.1 (1.0)	128 ± 3.8 (1.0)	136 ± 4.7 (1.0)
	2000	29 ± 3.1 (1.0)	35 ± 2.3 (1.1)	129 ± 3.1 (1.0)	140 ± 8.5 (1.0)
	4000	30 ± 1.5 (1.1)	33 ± 3.5 (1.0)	124 ± 4.7 (1.0)	135 ± 4.4 (1.0)
PCO 300 min	0	29 ± 3.5	35 ± 2.6	126 ± 8.7	138 ± 3.8
	500	30 ± 3.6 (1.0)	36 ± 6.8 (1.0)	124 ± 5.9 (1.0)	133 ± 8.1 (1.0)
	1000	31 ± 2.3 (1.1)	36 ± 1.5 (1.0)	125 ± 4.6 (1.0)	136 ± 4.0 (1.0)
	2000	27 ± 4.5 (0.9)	32 ± 3.0 (0.9)	127 ± 4.9 (1.0)	141 ± 6.1 (1.0)
	4000	27 ± 4.7 (0.9)	36 ± 3.5 (1.0)	124 ± 4.0 (1.0)	139 ± 3.0 (1.0)
Solvent control[c]	100	28 ± 3.5	37 ± 2.0	126 ± 5.7	137 ± 3.1
Positive control[d]	50	1264 ± 52.4 (45.1)		602 ± 25.5 (4.8)	
	20		2973 ± 72.5 (80.4)		1148 ± 44.5 (8.4)

[a] Mean ± standard deviation.
[b] Negative control.
[c] DMSO only.
[d] 50 μg plate^{-1} Dexon without S9 and 20 μg plate^{-1} 2-aminofluorene with S9.

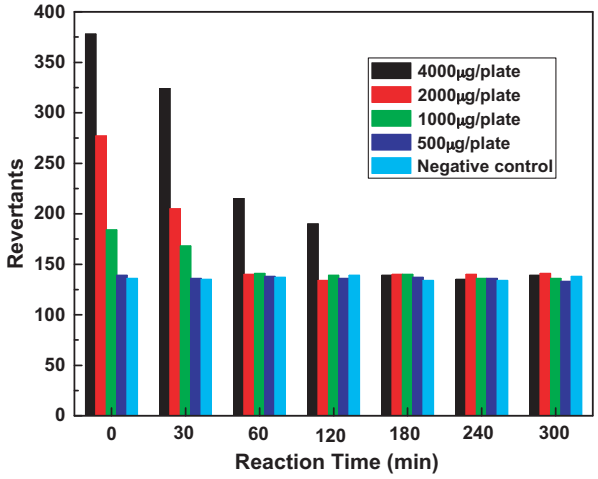

Fig. 8. The mutagenicity intensity to TA100 (+S9) at different tested doses of raw o-ClA and gaseous intermediates at different degradation intervals.

curve. At different degradation intervals of 30, 60, 120, 180, 240, and 300 min, the MI values were all less than 2, and the results were all negative to strain TA98 with or without S9 in all dose groups of 4000, 2000, 1000, and 500 μg plate^{-1}, indicating that the intermediates in the gaseous phase do not cause base frameshift-type mutagenicity to organisms. In addition, compared with the negative control in all dose groups, no increase in the number of revertants per plate was detected for strain TA100 without S9. However, different results were obtained for strain TA100 with S9. At the 30 min interval, the number of revertants per plate was 324 ± 7.2 (MI = 2.4) at 4000 μg plate^{-1} and 205 ± 10.3 (MI = 1.5) at 2000 μg plate^{-1}, indicating that the gaseous intermediates have a weak mutagenicity to strain TA100 at 4000 μg plate^{-1} with S9 activation. The number of revertants per plate obtained for strain TA 100 with S9 decreased rapidly after 60 min, and the MI values were all less than 2, suggesting that the intermediates with mutagenicity can be subsequently photocatalytically degraded into less mutagenic intermediates. To illustrate clearly the detoxification capability of photocatalytic technology at different degradation intervals, the histogram of mutagenicity intensity to TA100 (+S9) at 4000, 2000, 1000, and 500 μg plate^{-1} is shown in Fig. 8. The profiles of the mutagenic toxicity for TA100 (+S9) decreased rapidly with an increase in degradation time at all four doses. The number of revertants per plate is near the spontaneous reversions in all doses after a 180 min reaction. This indicates that the degradation of the gaseous mixed intermediates of *o*-ClA did not show any mutagenicity. The same change trend was obtained in the SOS/umu assay, except that the gaseous mixed intermediates after a 30 min degradation showed weak mutagenicity to TA100 (+S9) at a high dose of 4000 μg plate^{-1}. The results of both SOS/umu assay and Ames test indicated that photocatalytic technology had an excellent capability to decontaminate *o*-ClA efficiently, and the gaseous degradation mixture did not exhibit mutagenicity to human health after 180 min degradation, although the Ames test can obtain more plausible results than the SOS/umu assay.

4. Conclusions

The photocatalytic degradation kinetics of *o*-ClA was investigated, and it was found to follow a pseudo first-order reaction. The resulting lower rate constant and longer half-life indicated that *o*-ClA was difficult to degrade by photocatalytic technology. Two less toxic gaseous intermediates (chlorobenzene and phenol) and trace solid phenol and o-dihydroxybenzene on the surface of TiO_2 were found during the course of degradation, although the photocatalytic degradation efficiencies can reach as high as 99.0% within a 300 min illumination. The results of both SOS/umu assay and Ames test indicated that photocatalytic technology had excellent capability to decontaminate *o*-ClA efficiently, and the gaseous degradation mixture did not exhibit mutagenicity to human health after a 180 min degradation.

Acknowledgements

This is contribution No. IS-1268 from GIGCAS. This work was financially supported by Science and Technology Project of Guangdong Province, China (2007A032301002, 2009B030400001 2009A030902003 and 2006A36701002) and NSFC (40572173)

Appendix A. Supplementary data

Supplementary data associated with this article can be found, in the online version, at doi:10.1016/j.apcatb.2010.11.035.

References

[1] J. Jeong, K. Sekiguchi, K. Sakamoto, Chemosphere 57 (2004) 663–671.
[2] K.R. Jones, N. Brautbar, Toxicol. Ind. Health 13 (1997) 743–750.
[3] C.P. Rennix, M.M. Quinn, P.J. Amoroso, E.A. Eisen, D.H. Wegman, Am. J. Ind. Med. 48 (2005) 157–167.
[4] C.T. Chang, B.Y. Chen, J. Hazard. Mater. 153 (2008) 1262–1269.
[5] H. Ben Mansour, D. Barillier, D. Corroler, K. Ghedira, L. Chekir-Ghedira, R. Mosrati, Environ. Toxicol. Chem. 28 (2009) 489–495.
[6] C. Wang, J.Y. Xi, H.Y. Hu, Chemosphere 73 (2008) 1167–1171.
[7] E. Dybing, J. O'Brien, A.G. Renwick, T. Sanner, Toxicol. Lett. 180 (2008) 110–117.
[8] R.J. Brennan, R.H. Schiestl, Mutat. Res. 430 (1999) 37–45.
[9] M.J. O'Neil, The Merck Index: An Encyclopedia of Chemicals, Drugs and Biologicals, 14th Ed., Merck & Co. Inc, 2006.
[10] USEPA, National Emission Standard for Hazardous Air Pollutants (1985).
[11] T.C. An, L. Sun, G.Y. Li, S.G. Wan, J.M. Fu, G.Y. Sheng, J. Mol. Catal. A-Chem. 333 (2010) 128–135.
[12] H. Radianingtyas, G.K. Robinson, A.T. Bull, Appl. Microbiol. Biotechnol. 62 (2003) 423–429.
[13] L.L. Zhang, D. He, J.M. Chen, Y. Liu, J. Hazard. Mater. 179 (2010) 875–882.
[14] W.K. Choy, W. Chu, Ind. Eng. Chem. Res. 46 (2007) 4740–4746.
[15] F. Gosetti, M. Bottaro, V. Gianotti, E. Mazzucco, P. Frascarolo, D. Zampieri, C. Oliveri, A. Viarengo, M.C. Gennaro, Environ. Pollut. 158 (2010) 592–598.
[16] G. Mailhot, L. Hykrdova, J. Jirkovsky, K. Lemr, G. Grabner, M.B. Bolte, Appl. Catal. B-Environ. 50 (2004) 25–35.
[17] M.L. Zhang, T.C. An, J.M. Fu, G.Y. Sheng, X.M. Wang, X.H. Hu, X.J. Ding, Chemosphere 64 (2006) 423–431.
[18] J.M. Stokke, D.W. Mazyck, Environ. Sci. Technol. 42 (2008) 3808–3813.
[19] T.C. An, G.Y. Li, X.H. Zhu, J.M. Fu, G.Y. Sheng, Z. Kun, Appl. Catal. A-Gen. 279 (2005) 247–256.
[20] J. Zhao, X.D. Yang, Build. Environ. 38 (2003) 645–654.
[21] L. Sun, T.C. An, S.G. Wan, G.Y. Li, N.Z. Bao, X.H. Hu, J.M. Fu, G.Y. Sheng, Sep. Purif. Technol. 68 (2009) 83–89.
[22] L. Sun, G.Y. Li, S.G. Wan, T.C. An, J.M. Fu, G.Y. Sheng, Chemosphere 78 (2010) 313–318.
[23] X. Zhang, F. Wu, X.W. Wu, P.Y. Chen, N.S. Deng, J. Hazard. Mater. 157 (2008) 300–307.
[24] T.C. An, H. Yang, G.Y. Li, W.H. Song, W.J. Cooper, X.P. Nie, Appl. Catal. B-Environ. 94 (2010) 288–294.
[25] S. Horikoshi, N. Serpone, J.C. Zhao, H. Hidaka, J. Photochem. Photobiol. A-Chem. 118 (1998) 123–129.
[26] Y. Oda, S. Nakamura, I. Oki, T. Kato, H. Shinagawa, Mutat. Res. 147 (1985) 219–229.
[27] E. Wittekindt, B. Fischer, P.D. Hansen, ISO/DIS 13829 (2000) 39–57.
[28] J. Li, M. Ma, Q. Cui, Z.J. Wang, Bull. Environ. Contam. Toxicol. 80 (2008) 492–496.
[29] D.M. Maron, B.N. Ames, Mutat. Res. 113 (1983) 173–215.
[30] G.Y. Li, T.C. An, X.P. Nie, G.Y. Sheng, X.Y. Zeng, J.M. Fu, Z. Lin, E.Y. Zeng, Environ. Toxicol. Chem. 26 (2007) 416–423.
[31] M.R. Hoffmann, S.T. Martin, W.Y. Choi, D.W. Bahnemann, Chem. Rev. 95 (1995) 69–96.
[32] X.L. Zhu, C.W. Yuan, Y.C. Bao, J.H. Yang, Y.Z. Wu, J. Mol. Catal. A-Chem. 229 (2005) 95–105.
[33] Y. Ohko, K.I. Iuchi, C. Niwa, T. Tatsuma, T. Nakashima, T. Iguchi, Y. Kubota, A. Fujishima, Environ. Sci. Technol. 36 (2002) 4175–4181.
[34] W.K. Choy, W. Chu, Chem. Eng. J. 136 (2008) 180–187.
[35] J. Bandara, J.A. Mielczarski, A. Lopez, J. Kiwi, Appl. Catal. B-Environ. 34 (2001) 321–333.
[36] S. Ishikawa, K. Baba, Y. Hanada, Y. Uchimura, K. Kido, Bull. Environ. Contam. Toxicol. 42 (1989) 65–70.
[37] S. Nakamura, Y. Oda, A. Nakata, H. Shinagawa, Mutat. Res. 147 (1985), 267–267.
[38] L.D. Claxton, P.P. Matthews, S.H. Warren, Mutat. Res. 567 (2004) 347–399.